Available online at www.sciencedirect.com
SCIENCE DIRECT
Carbohydrate Research 340 (2005) 2761–2772
Carbohydrate RESEARCH

The structure of the lipopolysaccharide from a *galU* mutant of *Pseudomonas aeruginosa* serogroup-O11

Biswa Choudhury,[a] Russell W. Carlson[a,*] and Joanna B. Goldberg[b]

[a]*Complex Carbohydrate Research Center, 315 Riverbend Road, University of Georgia, Athens, GA 30602, United States*
[b]*Department of Microbiology, University of Virginia, Charlottesville, VA 22908, United States*

Received 23 December 2004; accepted 15 September 2005
Available online 17 October 2005

Abstract—The lipopolysaccharide (LPS) of a *galU* mutant of *Pseudomonas aeruginosa* PA103, a serogroup O11 strain, was sequentially extracted with phenol–chloroform–petroleum ether (PCP) followed by hot phenol–water extraction of the bacterial pellet remaining after PCP extraction. LPS was found in both the PCP extract as well as in the water phase of the hot phenol–water extract. Analysis of the carbohydrate portion released by mild acid hydrolysis of both LPS preparations, both before and after removal of all phosphate groups by treatment with aqueous HF, was performed by glycosyl composition and linkage analyses as well as by NMR and mass spectrometric analyses. The results showed that the carbohydrate portion of these two LPS extracts contained the same structure: namely, α-GalN(Ala)-(1→3)-α-(7-Cm)HepII-(1→3)-α-HepI-(1→5)-α-Kdo-(2→. The oligosaccharide preparation from PCP-extracted LPS consisted of a variety of structures containing up to six phosphate groups present as mono-, pyro-, and possibly triphosphate, primarily located on the HepI residue with some molecules having a monophosphate on HepII. The oligosaccharide preparation from the hot phenol–water-extracted LPS contained a similar variety of structures, but with an additional structure in which HepI contained a PPEA group at O-2. In addition, PAGE immunoblot analysis of the crude cellular extract with anti-A-antibodies revealed the presence of A-band material in both PA103 and the *galU* mutant. The A-band material was purified and characterized by glycosyl composition and linkage analyses, as well as by NMR spectroscopy, which confirmed that the A-band rhamnan polysaccharide was present but not as typical LPS since lipid-A or LPS core oligosaccharide components were not detected.

Keywords: *Pseudomonas aeruginosa*; Lipopolysaccharide; Inner core; *galU*, Biosynthesis

1. Introduction

Pseudomonas aeruginosa is an opportunistic pathogen most frequently isolated from chronically infected cystic fibrosis patients and nosocomial infections. It is a major threat to immune-compromised patients. It is also the most likely pathogen found in ulcerative keratitis in individuals with extended use of contact lens. This organism is highly adaptable for survival in a wide range of environments.

As with other Gram-negative bacteria, the lipopolysaccharide (LPS) of *P. aeruginosa* is a major virulence factor and is also reported to be the most immunogenic among the various *P. aeruginosa* cell-surface antigens.[1] The LPS from different serogroups of *P. aeruginosa* possess the same general architecture as those from the family Enterobacteriaceae being composed of lipid-A, a core oligosaccharide, and serologically distinct O-antigenic polysaccharides. The core oligosaccharide is further divided into a relatively conserved inner core and a distal and slightly variable outer core region as was shown by several monoclonal antibody binding assays.[2] *P. aeruginosa* strains produce two antigenically and chemically distinct LPS molecules; namely A-band and B-band LPS. The A-band LPS is a neutral polysaccharide consisting of one α-(1→2)- and two α-(1→3)-linked D-rhamnosyl units, which is antigenically conserved and

* Corresponding author. Tel.: +1 706 542 4439; fax: +1 706 542 4412; e-mail: rcarlson@ccrc.uga.edu

0008-6215/$ - see front matter © 2005 Elsevier Ltd. All rights reserved.
doi:10.1016/j.carres.2005.09.017

known as the common antigen (CA).[3] In contrast, B-band LPSs possess O-antigen polysaccharides that consist of various hetero-oligosaccharide repeating units.[4] The diverse chemical nature of the B-band O-antigen polysaccharides is the basis for the serotype classification of this organism. According to the International Antigen Typing Scheme (IATS) and the Lanyi–Bergan classification, all known *P. aeruginosa* strains have been placed into 30 different serotypes.[4]

Most of the *P. aeruginosa* strains are highly resistant to common antibiotics and antiseptics. The resistance of enteric bacteria to these molecules is considered to be associated with a high phosphate content in the LPS inner core region.[5] Interestingly, isolates of *P. aeruginosa* recovered from the environment and from nosocomial infections contain smooth LPSs (i.e., LPSs containing the O-antigen polysaccharide) and are serum resistant, while those from the lung of cystic fibrosis patients are rough-type LPSs that lack the O-antigen.[6] It was also shown that the LPS outer core of *P. aeruginosa* is necessary for both pneumonia and corneal infections in a mouse model.[7] The cystic fibrosis transmembrane conductance regulator (CFTR) molecule on the host cell recognizes the outer core oligosaccharide, promotes internalization of the organism by epithelial cells and the subsequent presentation of *P. aeruginosa* cells to the host immune system for clearance.[8] In order to fully understand the role of LPS in determining the virulence of *P. aeruginosa*, it is necessary to characterize the biosynthesis of this molecule and the structures of LPS from defined mutants that are affected in their pathogenicity. In addition, because of the serological diversity of *P. aeruginosa*, LPSs and the chemical changes that occur during infection, there is interest in developing an immunotherapy based on a structural region of the LPS that is conserved across a broad spectrum of the various *P. aeruginosa* serogroups. Therefore, it is necessary to characterize the structures of the LPS inner core regions for the different *P. aeruginosa* serogroups.

The conserved carbohydrate structure found within the inner core region of *P. aeruginosa* LPSs consists of →α-GalN-(1→3)-α-HepII (7-Cm)-(1→3)-α-HepI-(1→5)-α-Kdo-(2→ in which GalN is either *N*-acetylated or *N*-alanylated and the HepI and HepII residues are variably phosphorylated.[9] The core region of a rough LPS from clinical isolate 2192 was shown to have the above inner core structure in which GalN was *N*-alanylated, HepII substituted with monophosphate at O-4 and O-6, and HepI substituted with monophosphate at O-2 and O-4.[10] The inner core region of a serogroup O-12 strain was shown to have HepII phosphorylated at O-6, and HepI at both O-2 and O-4.[11] This monophosphate substitution pattern was also reported for the core region of an immunotype 1 lipopolysaccharide.[12] Recently, the inner core structure for a serogroup O5 Δ*algC* mutant of PA01 was reported showing that HepI contains a pyrophosphoethanol amine (PPEA) group at O-2, and HepII is phosphorylated at O-6.[13] That report also describes the inner core of an O3 serogroup mutant, PAC1R, as having phosphates at O-2 and O-4 of HepI and at O-6 of HepII, with HepII also being carbamoylated at O-7, and the GalN residue containing an *N*-alanyl group. In addition, it was shown that the LPS from the serogroup O5 parent PAO1 contained two phosphates on HepI (at O-2 and O-4) and one phosphate on HepII (at O-6). The above work indicates variability in the location of phosphate groups in the inner core structures from serogroups O6 and O5; for example, either one, two, or three phosphate groups on HepI, one phosphate on HepII, or phosphate and PPEA groups on HepI and one phosphate on HepII. Some of this variability may be related to differences among serogroups, or to the possibility that some deep rough mutants may have an altered phosphorylation pattern compared to the inner core region of their respective parent strains.

In addition to the effects on alginate production and alteration in LPS structure, the PAO1 *algC*::tet mutant was noted to have a slower growth rate.[14] However, despite these pleoitropic effects, the studies on the pathogenesis of the *algC* mutant have been informative. As anticipated, due to its altered LPS, the PAO1 *algC*::tet was much more sensitive to the effects of normal human serum compared to its parental strain.[15] In a murine corneal infection model, this mutant was virtually avirulent, showing about $<3\log_{10}$ difference in the ID_{50} compared to the parental strain. Similarly, the mutant was avirulent in a burned mouse model and showed no disseminated from the site of infection after thermal injury.[14] The *algC* mutant was much less virulent in a neonatal mouse model of pneumonia and showed very low levels of bacteria in the lungs and spleen of these mice corresponding to colonization and bactermeia, respectively.[16]

The studies of the virulence of *galU* mutants have just been published;[17] *galU* mutants of the serogroup O5 strain PAO1 and serogroup O11 PA103 (the subject of this report) were compared to their respective parental strains. Distinct from that observed for the *algC* mutant, neither of the *galU* mutants had any apparent in vitro growth defect. Both mutants were much more serum sensitive. Also, similar to what was observed for the *algC* mutant in mouse corneal infection, both the *galU* mutants were avirulent and showed a $2–4\log_{10}$ increase in the ID_{50}. With respect to lethality in a murine acute pneumonia model, the *galU* mutants were significantly attenuated resulting in an LD_{50} $1–1.4\log_{10}$ above that of the corresponding wild-type strain. The level of bacterial colonization was measured in mice after intranasal infection with the wild-type and *galU* mutants. Even 1 h after infection, there were significantly fewer bacteria in the lung of mice infected with PAO1 *galU* compared to PAO1; 20 h after infection, this difference was even more

dramatic. However, for mice infected with PA103 and its *galU* mutant, similar bacterial loads were seen in the lungs of mice 6 h after infection. In both cases, the *galU* mutants were never completely cleared from the lung, but neither *galU* mutant ever disseminated to the spleen after intranasal infection. These findings indicate that a complete LPS is not required for survival in the respiratory tract but is required for dissemination.[17]

Here, we report the chemical structure of LPS from the *galU* mutant of PA103, a strain belonging to serogroup O11. The mutation in the *galU* gene blocks the biosynthesis of UDP-glucose from glucose-1-P, a precursor needed for the glucosyl residues found in the outer core of PA103 LPS.[17,18] The *galU* mutant produces a rough LPS with a truncated core oligosaccharide as did the PAO1 *algC*::tet,[18] but contains a larger variety of structures varying in the number and location of phosphate, pyrophosphate, triphosphate, and PPEA groups. We also noted that the *galU* mutant produces A-band reactive material, while it was previously noted that PAO1 *algC*::tet did not express this type of LPS.[15] The *galU* mutant also differs from the *algC* mutant in that it produces mucoid material,[18] presumably alginate, while the PAO1 *algC*::tet did not produce alginate.

2. Experimental

2.1. Preparation of the lipopolysaccharide fractions

The bacterial cultures were prepared as previously described.[19] The cell pellet of the *galU* mutant was washed with distilled water and centrifuged at 10,000 rpm, 10 °C for 15 min to remove adhered media. The packed cells were washed with 95% ethanol (twice), acetone (twice) and diethyl ether (once), and dried under vacuum over P_2O_5. LPS was extracted from dried and finely ground cells by phenol–chloroform–petroleum ether (PCP) extraction.[20] After removal of the chloroform and petroleum ether, the LPS was precipitated by the dropwise addition of water. The precipitated LPS was collected by low speed centrifugation and washed once with 80% phenol and several times with a 1:1 diethyl ether–acetone mixture to remove any phenol. Finally, the phenol-free LPS was suspended in deionized water and collected by centrifugation at 20,000 rpm, at 10 °C for 1 h. This centrifugation step was repeated, and the final precipitate was suspended in water and lyophilized. This LPS preparation is hereafter referred to as LPS-PCP.

Hot phenol–water extraction[21] was done on the bacterial residue remaining after the above PCP extraction. This bacterial residue was washed several times with a 1:1 mixture of diethyl ether and acetone and then extracted with hot phenol–water. The material extracted into the water phase was further purified by treatment with ribo- and deoxyribonucleases and proteinase K. The solution was then dialyzed and lyophilized. A 1% aqueous solution of this material was ultracentrifuged at 120,000*g* for 4 h at 5 °C. The precipitate was resuspended in water and again ultracentrifuged. The supernatants were pooled and lyophilized, and the precipitate contained the LPS, hereafter referred to as LPS-W. The material in the supernatant was enriched in rhamnose (see Section 3 below) and this rhamnose-containing material was further purified by gel-permeation chromatography using a Bio-Gel P10 column. In addition, this material was also treated with 1% acetic acid at 100 °C for 1.5 h and again subjected to gel-permeation chromatography using Bio-Gel P10.

2.2. DOC–PAGE

LPS samples were suspended in water at 2 μg/μL, dissolved in a 1:1 ratio with electrophoresis sample buffer and separated on a 18%-polyacrylamide gel containing deoxycholate (DOC) as the detergent.[22] The electrophoresis was performed at a constant current of 30 mA. The gel was fixed in an aqueous solution containing 40% ethanol and 5% acetic acid. Finally, the gel was stained using a Bio-Rad silver staining kit following the method of Tsai and Frasch.[23]

2.3. Western blot analysis with anti-A antibodies

Cells were extracted as described previously.[24] Cell extract samples were separated on a 12% acrylamide–SDS-PAGE. Western immunoblot analyses were performed as described previously[24] using monoclonal antibody N1F10 specific for A-band LPS.[25] Blots were developed with anti-mouse IgM-alkaline phosphatase (Roche). Sigma FAST BCIP/NBT (5-bromo-4-chloro-3-indolyl phosphate–nitroblue tetrazolium) tablets (Sigma, cat. no. B5655) were used as the alkaline phosphatase substrate as specified by the manufacturer.

2.4. Isolation and modification of the core oligosaccharide

The oligosaccharide (OS) was released from LPS-PCP and LPS-W by mild acid hydrolysis using 1% HOAc at 100 °C for 1.5 h to give OS-PCP and OS-W, respectively. The lipid-A precipitate was removed by low-speed centrifugation, and the supernatant was fractionated on a Bio-Gel P2 column using water as the eluent. The eluent was continuously monitored using an RI-detector, and the OS fractions were pooled and lyophilized. The OS eluted at about 1.5 times the excluded volume of the column, and a second fraction eluted near the included volume. Dephosphorylation of the OS was performed by treatment with 48% HF at 4 °C for 48 h.[26] The HF was neutralized carefully with 1 M ammonium hydroxide below 0 °C, and the neutralized material was desalted on a Bio-Gel P2 column.

Oligosaccharides obtained from the mild acid hydrolysis of LPS-W were also separated by gel-filtration chromatography using Bio-Gel P4 (fine). This procedure allowed the separation of oligosaccharides containing PEA from those lacking PEA (described in the Results section below).

2.5. Composition analysis of core oligosaccharide

LPS and oligosaccharide fractions were methanolyzed by methanolic 1 M HCl at 80 °C for 18 h, followed by N-reacetylation of the methyl glycosides using pyridine–Ac_2O in the presence of MeOH at 100 °C for 1 h. The free hydroxyl groups of N-reacetylated methyl-glycosides were trimethylsilylated using Tri-Sil reagent (Pierce) at 80 °C for 20 min. The volatile methyl per-*O*-trimethylsilylglycosides (per-*O*-TMS-glycosides) were then analyzed by combined gas chromatography–mass spectrometry (GC–MS) equipped with a mass-selective detector using a DB-1 capillary column (Hewlett–Packard HP 5890 GC interfaced to a 5970 MSD).[27] The fatty acids and hydroxy fatty acids were also detected as their methyl esters by GC–MS during this same analysis.

2.6. Glycosyl linkage analysis

Linkage analysis was performed by the preparation and GC–MS analysis of partially methylated alditol acetates (PMAAs). The PMAAs were prepared using the method of Ciucannu and Kerek.[28]

2.7. NMR spectroscopy

NMR spectra were collected on a Varian Inova 500 spectrometer using software supplied by Varian, and the data were processed using NMRpipe and NMRdraw software. The samples were exchanged several times with D_2O (99.8% Aldrich) and final measurements were made in 0.5 mL D_2O solutions (100% D; Cambridge Isotope Laboratories) at 27 °C. ^1H NMR spectra were measured at 500 MHz using a spectral width of 8 kHz. The gCOSY spectra were measured over a spectral width of 2.2 kHz using a dataset of $(t_1 \times t_2)$ of 256×2048 points with 16 scans. The TOCSY spectrum was collected using the same sized data set with 32 scans utilizing a mixing time of 80 ms. For the HSQC experiment, the spectral widths in the ^1H and ^{13}C dimensions were 2.2 and 13.9 kHz, respectively, and 96 scans were acquired. The multiple-bond correlation (HMBC) experiment was performed with 128 scans, and the spectral widths were set at 2.2 and 22.0 kHz in the ^1H and ^{13}C dimensions, respectively. ^{31}P NMR spectra were measured at 202.38 MHz by employing a spectral width of 5 kHz, with phosphoric acid (85%) as the external standard ($\delta_p = 0.0$ ppm).

^1H detected ^1H–^{31}P HMQC and HMQC-TOCSY experiments were done on a Varian 500 spectrometer according to the standard pulse sequence supplied by Varian. Spectra were acquired using the spectral width of 5 kHz in ^{31}P dimension and 2.2 kHz in the ^1H dimension.

2.8. Mass spectrometry

For MALDI-TOF MS the OS samples were dissolved in deionized water (1 μg/μL), mixed with 0.5 M 2,5-dihydroxybenzoic acid (DHB) in a 1:1 (v/v) ratio and spotted on a stainless steel plate. The phosphorylated OS, however, responded better in the negative-ion mode using 0.5 M 3-aminoquinoline as matrix in a 1:1 (v/v) sample to matrix ratio. The collision-induced decay (CID) was performed using air as the collision gas on an Applied Biosystems 4700 Proteomics Analyzer MALDI TOF/TOF instrument. The electrospray-ionization mass spectrometry (ESIMS) and in-source fragmentation experiments were done on an ion-trap LCQMS instrument from Thermo-Finnigan, using helium as the buffering and target gas.

3. Results

3.1. Analysis of the PCP-extracted LPS (LPS-PCP)

The yield of LPS-PCP isolated from the *galU* mutant by phenol–chloroform petroleum ether extraction method was 6.2% of the dried bacterial cell pellet. DOC–PAGE analysis (Fig. 1) of isolated LPS-PCP showed two low molecular weight bands migrating near the electrical front. The LPS-PCP bands from the *galU* mutant had faster electrophoretic mobilities compared to the LPS bands from the parent strain, PA103, clearly indicating that the *galU* mutant has a defect in the biosynthesis of the core portion of the LPS-PCP. The occurrence of two bands in the PAGE analysis of the *galU* LOS may reflect the heterogeneity in the core oligosaccharide which is described further below. Figure 1B shows that crude SDS cell extracts from both the parents and the *galU* mutant contain anti-A-band reactive material. Therefore, it was important to characterize this A-band material from the *galU* mutant (this characterization is described below). The A-band material was not found in the purified LPS preparations from the *galU* mutant (described further below).

Glycosyl composition analysis of the LPS-PCP isolated from the *galU* mutant showed the presence of galactosamine (GalN), glucosamine (GlcN), and Kdo. The presence of heptose (Hep) could only be confirmed in GC–MS after dephosphorylation of the sample. Analysis of LPS-PCP also indicated the presence of lauric acid (C12:0), β-hydroxydecanoic acid (β-OH-C10:0),

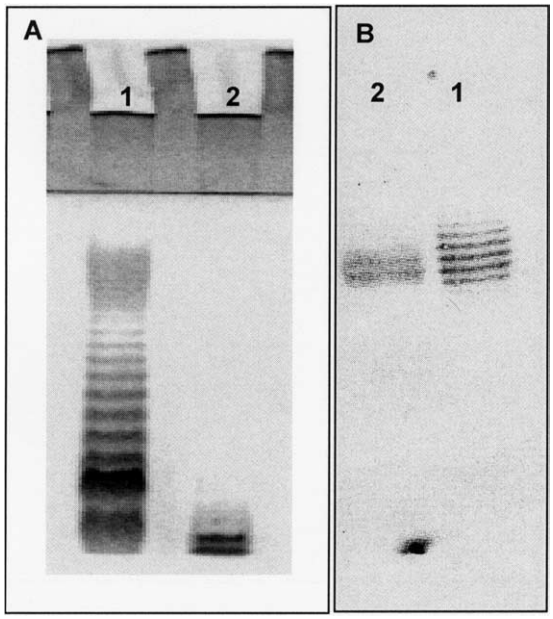

Figure 1. (A) DOC–PAGE analysis of the purified LPS-PCP preparations from the PA103 parent (well 1), and PA103 *galU* mutant (well 2) cells. (B) A DOC–PAGE immunoblot of the SDS-cell extract from the PA103 parent (well 1), and PA103 *galU* mutant (well 2) cells. The immunoblot was developed using anti-A-band monoclonal antibody.

β-hydroxylauric acid (3-OH-C12:0) and α-hydroxylauric (2-OH-C12:0) acid as the lipid-A fatty acyl components. The absence of rhamnose (Rha), glucose (Glc) and *N*-acetylfucosamine (FucNAc) was a clear indication that the purified LPS-PCP preparation lacked both A- and B-band O-chain polysaccharide and consisted of an inner-core OS attached to the lipid-A. This finding was consistent with the DOC–PAGE profile described above.

The oligosaccharide, OS-PCP, was prepared from LPS-PCP by mild acid hydrolysis, and the lipid-A was removed by low speed centrifugation. The supernatant was further purified by size-exclusion column chromatography using Bio-Gel P2. The major fraction (OS-PCP) eluted as a single peak in the partially included volume, and a minor second fraction eluting near the included volume was identified as Kdo.

The glycosyl composition of OS-PCP indicated the presence of GalN, Kdo and a trace amount of Hep. However, the exact ratio of the sugar constituents was obtained only after dephosphorylation of this OS since accurate quantification of phosphorylated residues could only be accomplished after the removal of the phosphate groups. Composition analysis of dephosphorylated OS showed a GalN:Hep:Kdo ratio of 1.0:1.8:1.0. Again, the absence of any Rha, Glc, and FucNAc was a clear indication of the absence of both A-band and B-band O-chain polysaccharide, as well as the absence of an outer core oligosaccharide.

The carbohydrate structure of the OS-PCP was determined by NMR and MS analysis of the HF-treated OS-PCP sample. The proton assignment of each glycosyl residue of OS-PCP was determined through gCOSY and TOCSY experiments (spectra not shown), and the results are given in Table 1. The ^{13}C assignments were obtained from a ^{1}H–^{13}C one bond correlated gHSQC experiment (spectrum not shown), and the results are also given in Table 1. The sequence of the glycosyl residues in the OS was established from an HMBC experiment, which revealed through-bond transglycosidic connections. The results of the HMBC experiment showed that H-1 of the GalN(Ala) residue is correlated to the C-3 of HepII (5.26→79.5). Similarly, the HepII anomeric proton shows connectivity with the C-3 of HepI (5.16→80.2), and H-1 of HepI shows a correlation with C-5 of Kdo (5.08→76.1). In addition, the HMBC spectrum showed a correlation between the methyl protons of alanine (1.50 ppm) with its carbonyl carbon (174.0 ppm) and with C-2 of GalN (51.4 ppm), confirming the location of alanine on GalN. The carbonyl carbon of the carbamoyl moiety at 160.0 ppm shows a correlation to the H-7 methylene protons (4.25 and 4.04 ppm) of HepII, consistent with the location of carbamoyl group at this position. In summary, it was evident that the LPS biosynthesized by the *galU* mutant possess, a truncated core tetrasaccharide attached to the lipid-A moiety that has the structure, α-GalN(Ala)-(1→3)-α-(7-Cm)HepII-(1→3)-α-HepI-(1→5)-α-Kdo-(2→. This

Table 1. ^{1}H NMR and ^{13}C chemical shifts of the inner-core OS of *P. aeruginosa* serotypeO11 *galU* mutant

Residue	H-1/C-1	H-2/C-2	H-$3_{a,e}$/C-3	H-4/C-4	H-5/C-5	H-6_a, H-6_e/C-6	H-7/C-7	H-8/C-8
GalN	5.26 (100.5)	4.25 (51.4)	4.09 (67.4)	3.72 (70.5)	3.88 (72.4)	3.64, 3.88 (62.7)	—	—
HepII	5.16 (103.6)	4.27 (72.40)	4.02 (79.6)	3.71 (67.5)	3.79 (73.2)	4.13 (69.5)	4.25, 4.02 (65.5)	—
HepI	5.08 (102.4)	4.18 (68.0)	4.05 (80.2)	3.96 (67.0)	3.72 (72.9)	4.05 (65.5)	3.75, 3.65 (62.7)	—
Kdo	—	—	2.12, 1.87	4.10	4.14	3.78	3.85	3.60, 3.60
	174.0	(96.5)	(34.9)	(73.0)	(76.1)	(73.2)	(70.3)	(64.5)
Alanine	1.50 (3H, d, CH_3) (18.0), 4.08 (1H, q, α-CH), (50.5)							
Cm[a]	(160.0) (CONH_2)							

The carbon chemical shifts are given in parentheses.
[a] Cm = carbamoyl.

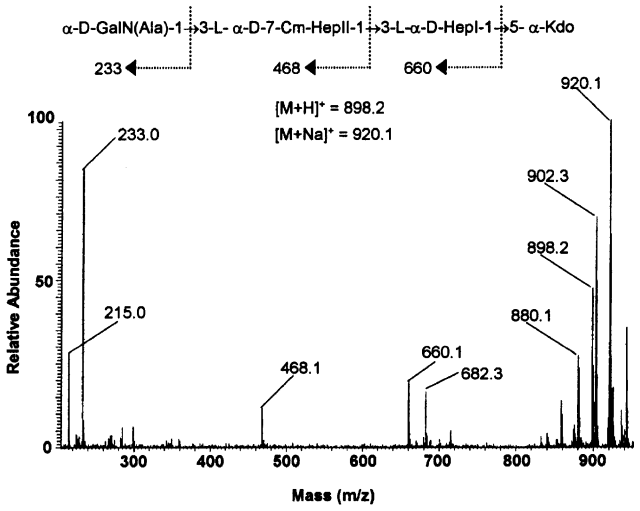

Figure 2. In-source fragmentation of dephosphorylated core-OS from *galU* mutant. The fragmentation pattern that gives rise to the various ions is shown.

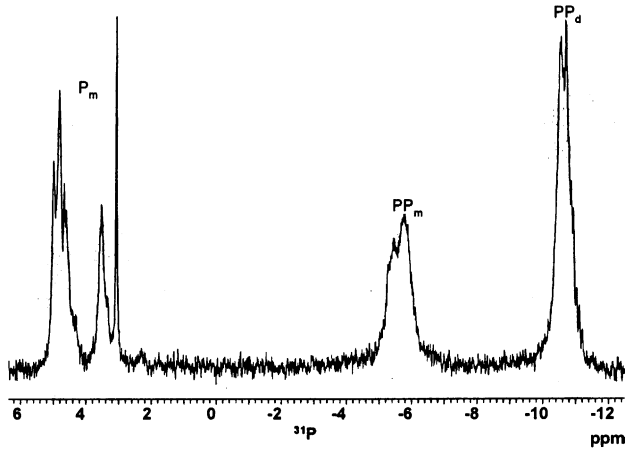

Figure 3. ^{31}P NMR spectrum of phosphorylated core oligosaccharide from the *galU* mutant LPS acquired at pH −9.0.

glycoside sequence is the same as that reported for the Δ*algC* mutant.[13]

The above structure of the OS in both dephosphorylated and native form was also supported by glycosyl-linkage and mass-spectrometric experiments. Methylation analysis of the dephosphorylated OS showed the presence of terminally linked GalN derived from GalN(Ala), 3-linked Hep and 5-linked Kdo residues. The ESIMS spectrum (Fig. 2) of the dephosphorylated OS showed the $[M+H]^+$ mass to be *m/z* 898.2, along with masses at *m/z* 880.1 (anhydro form), 920 ($[M+Na]^+$ form) and 902 (anhydro $[M+Na]^+$ form). The in-source fragmentation of the OS using a collision energy of 45 eV in an ion-trap instrument gave rise to several B-type ions. The *m/z* 233 fragment ion originates from the glycosyl oxonium ion of the non-reducing terminal GalN(Ala) residue, followed by the glycosyl oxonium ion with an additional mass increment of *m/z* 235 that is consistent with the addition of carbamoylated HepII [*m/z* 468 (B_2-ion)], a third fragment ion was at *m/z* of 660 indicating the next glycosyl residue to be the inner HepI (B_3-ion), and finally the Kdo residue gives the total mass of 897.

3.2. The location of phosphate groups on PCP-extracted LPS (LPS-PCP)

An important feature of the native OS was the presence of phosphate groups, which is a common feature of various *P. aeroginosa* core OSs (see Section 1). The ^{31}P NMR spectrum of the native OS-PCP indicated the presence of several phosphate groups including a signal around −10 ppm due to the presence of pyrophosphate groups. ^{31}P NMR analysis at higher pH (8.9) (Fig. 3) indicated the presence of both the P_α (−10 ppm) and P_β (−5.7 ppm) of the pyrophosphate groups, as well as downfield resonances due to monophosphate monoester groups. Mass spectrometric analysis, described in the next paragraph, indicated the possible presence of a triphosphate group in some of the structures. If present, such a group would show a ^{31}P signal at around −20 ppm. A resonance at this chemical shift was not observed indicating that another explanation exists for the mass spectrometric data, or that the molecule containing a triphosphate group is present in an amount that was below NMR-detectable levels.

The extent of phosphorylation heterogeneity and the location of the phosphate groups on OS-PCP were further investigated by mass spectrometric analysis. The MALDI-TOF MS spectra of the OS-PCP and OS-W (Fig. 4) indicated the presence of OSs bearing three (*m/z* 1136), four (*m/z* 1216), five (*m/z* 1296), and six (*m/z* 1376) phosphate groups, with the *m/z* 1136 ion

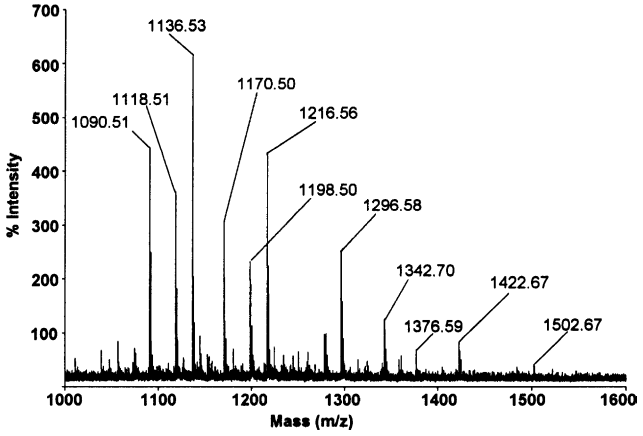

Figure 4. MALDI-TOF-MS of the phosphorylated core-OS from the *galU* mutant LPS. The proposed compositions for the various ions are shown in Table 2, with the exception of the minor ions of *m/z* 1242.7, 1422.7, and 1502.7, which remain unidentified.

having the greatest intensity. Ions were also observed for the anhydro Kdo forms of these molecules (e.g., *m/z* 1118, 1198, 1278, and 1358), as well as molecules containing 2-deoxyheptono-1,5-lactone, a degraded Kdo

Table 2. Observed masses and proposed compositions[a] for ions generated by negative-ion mode MALDI-TOF-MS on phosphorylated OS

Proposed structure	Observed (*m/z*)
[GalN(Ala)Hep(Cm)HepP$_3$Kdo–H]$^-$	1136.2
[GalN(Ala)Hep(Cm)HepP$_3$anhydroKdo–H]$^-$	1118.2
[GalN(Ala)Hep(Cm)HepP$_3$decarboxylactoneHep[b]–H]$^-$	1090.5
[GalN(Ala)Hep(Cm)HepP$_4$Kdo–H]$^-$	1216.2
[GalN(Ala)Hep(Cm)HepP$_4$anhydroKdo–H]$^-$	1198.2
[GalN(Ala)Hep(Cm)HepP$_4$ decarboxylactoneHep[b]–H]$^-$	1170.5
[GalN(Ala)Hep(Cm)HepP$_5$Kdo–H]$^-$	1296.2
[GalN(Ala)Hep(Cm)HepP$_5$anhydroKdo–H]$^-$	1278.1
[GalN(Ala)Hep(Cm)HepP$_6$Kdo–H]$^-$	1376.2
[GalN(Ala)Hep(Cm)HepP$_6$anhhydroKdo–H]$^-$	1358.1

[a] The compositions for the ions of *m/z* 1342.7, 1422.7, and 1502.7 shown in Figure 7 remain unknown. However, the mass difference of *m/z* 80 between these ions indicates that they differ from one another by a single monophosphate group.

[b] This is likely a 2-deoxyheptonic-1,5-lactone residue resulting from degradation of Kdo during mild acid hydrolysis as described by Olsthoorn et al.[32]

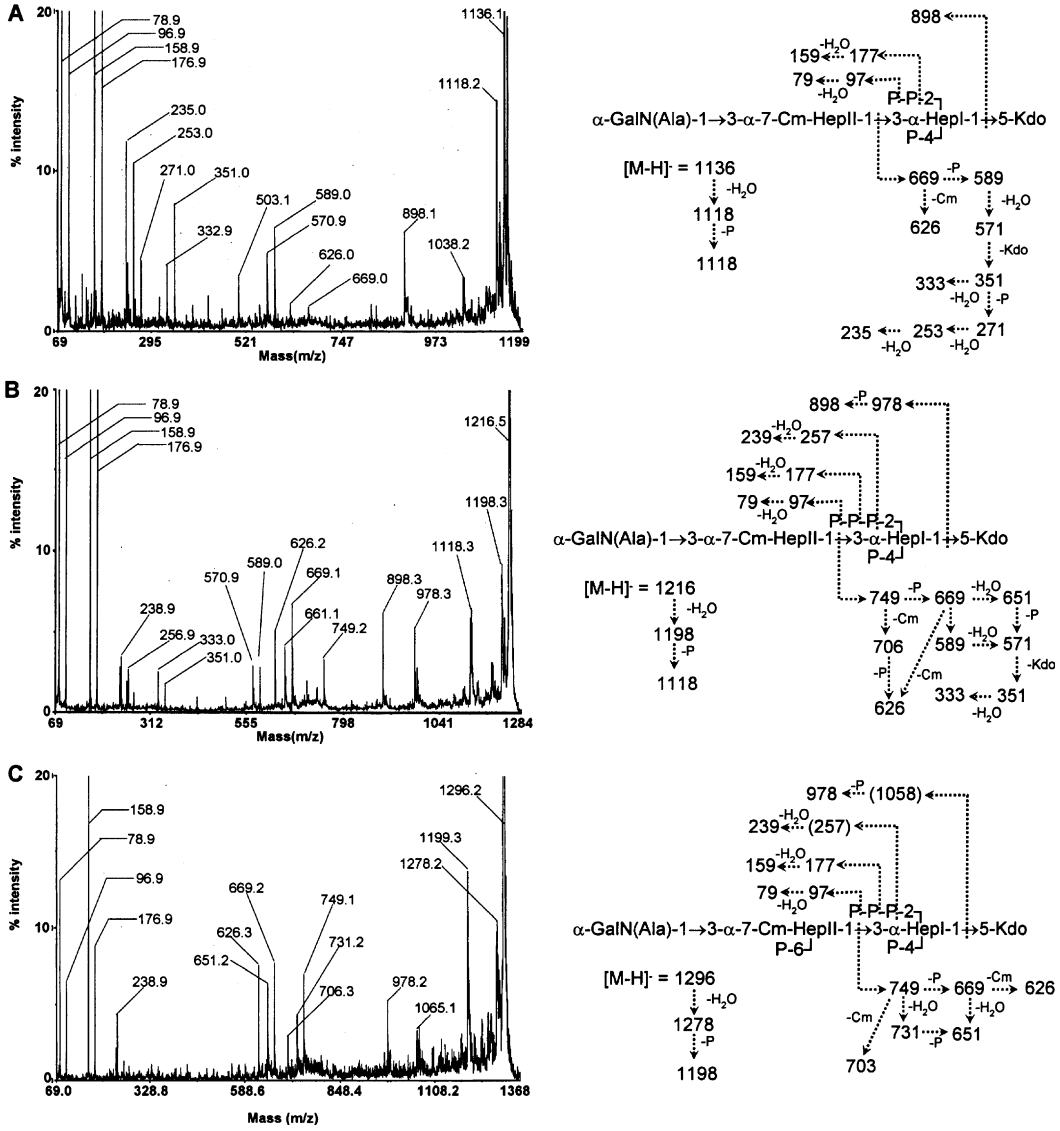

Figure 5. MALDI-TOF MS/MS spectra: (A) of ion 1136.1, (B) of ion 1216.1, and (C) of ion 1296. The fragmentation pattern is as indicated in the structures included with each ion.

residue resulting from the mild acid hydrolysis procedure[29] (i.e., a loss of 46 amu from ions of *m/z* 1090, and 1170). The proposed compositions for these ions are given in Table 2. Also a series of minor ions differing from each other by a single monophosphate group was also observed at *m/z* 1342, 1422, and 1502. The structures for these ions were not identified.

The CID-MS/MS spectra of the *m/z* 1136, 1216, and 1296 ions are shown in Figure 5 together with a structural diagram illustrating the possible source of the various fragment ions. The CID-MS/MS analysis of the *m/z* 1136.1 ion (Fig. 5a) gave rise to an Y_2 fragment of *m/z* 669.0, a result that is consistent with the location of three phosphate groups on the HepI residue. The loss of a phosphate group from the Y_2 fragment gives rise to an ion at *m/z* 589.0 and its anhydro form at *m/z* 570.9. Fragment ions were observed due to phosphate (*m/z* 96.9), and pyrophosphate (*m/z* 176.9). The B_3-ion at *m/z* 898.0 arises from the loss of Kdo. Fragment ions (e.g., Y_3 ions) indicative of phosphate on the HepII residue were not observed. Similarly, MS/MS analysis of the tetraphosphorylated OS (OS_{4P}) ion, *m/z* 1216 (Fig. 5b), also gave rise to B_3-ion due to the loss of Kdo (*m/z* 978.3). This fragment ion also loses a phosphate to give a mass of 898.3. The presence of Y_2-fragment with a mass of 749.2 indicates the presence of four phosphate groups on the HepI residue. The release of phosphate (*m/z* 78.9 and 96.9), pyrophosphate (*m/z* 158.9 and 176.9), and possibly triphosphate (*m/z* 238.9 and 256.9) was observed for this tetraphosphorylated species. As observed with MS/MS analysis of the *m/z* 1136 ion, fragments indicating phosphorylation of the HepII residue were not observed. MS/MS analysis of the pentaphosphorylated OS (OS_{5P}) ion, *m/z* 1296 is shown in Figure 5c. The presence of a Y_2-fragment with mass of 749.1 indicates the presence of four phosphate groups on the HepI residue. A Y_2 fragment ion due to five phosphates on HepI was not observed, suggesting the possibility that the fifth phosphate may be located on another glycosyl residue such as HepII. The presence of the fifth phosphate on HepII was indicated by a Y_3 fragment of *m/z* 1064.3 and, when run in the positive mode (not shown), a B2 ion of *m/z* 548, due to a GalN(Ala)-CmHepII(P) fragment.

In summary, the above data show that the OS-PCP structures consist of α-GalN(Ala)-(1→3)-α-(7-Cm)HepII($P_{0,1}$)-(1→3)-α-HepI($P_{3,4}$)-(1→5)-α-Kdo where the HepII residue can be non-phosphorylated or contain a single phosphate, and HepI can contain three phosphates as a monophosphate and a pyrophosphate (–P and –PP), or four phosphates as a monophosphate and triphosphate group (–P and –PPP) or two pyrophosphate groups. The locations of these phosphate groups were further determined by NMR analysis of the OS-W fractions as described below.

3.3. Structural analysis of the LPS isolated by hot phenol–water extraction (LPS-W)

In order to ensure a complete examination of all LPS forms present in this *galU* mutant, the LPS obtained by Westphal extraction was also characterized. The yield of this LPS (LPS-W) was 1.2% of dry bacterial cell weight. The DOC–PAGE of LPS indicated the presence of LPS with an electrophoretic mobility similar to that of LPS-PCP. The composition analysis after HF treatment showed the presence of GalN, Hep, and Kdo in the same ratio as observed for LPS-PCP. Fatty acids components were also the same as those observed for the LPS-PCP.

The core oligosaccharide (OS-W) was liberated by mild acid hydrolysis of LPS-W and eluted as a single peak in the partially included volume during Bio-Gel P2 gel-filtration chromatography. As with the OS-PCP sample, a second fraction eluted near the bed volume and was identified as monomeric Kdo. The linkage analysis of the HF-treated OS-W indicated the presence of terminally linked GalN and 3-linked Hep. The absence of Rha, Glc, and FucNAc supported the conclusion that the isolated OS-W did not contain either A- or B-band polysaccharide or the outer core oligosaccharide. These data also supported the conclusion that the glycosyl sequence of this oligosaccharide is the same as that described above for the HF-treated OS-PCP sample.

The OS-W was also analyzed by mass spectrometry. As with the OS-PCP sample, molecular ions were observed due to the presence of the tetrasaccharide containing from three to six phosphate groups; for example, $[M-H]^-$ ions with *m/z* of 1136.1, 1216, 1296, and 1376. This result shows that the OS-W fraction contained the same oligosaccharides as found in the OS-PCP fraction described above. However, unlike the OS-PCP sample, the OS-W sample contained an additional species with a molecular ion at *m/z* 1259.0, which is consistent with a triphosphorylated tetrasaccharide core with an additional PEA group. The *m/z* 1259 ion was particularly significant in intensity during ESIMS analysis (not shown) in comparison to MALDI-TOF-MS analysis. The presence of a PEA-containing component was also supported by a 1D ^{1}H NMR spectrum that showed a relatively strong signal at 3.22 ppm, indicating that the OS-W sample was comprised of a significant number of molecules containing PEA. This signal was absent from the ^{1}H NMR spectrum of the OS-PCP sample. As with the OS-PCP sample described above, ^{31}P NMR analysis showed the presence of both mono- and pyrophosphate groups.

In order to determine the probable location of the PEA signal, as well as the mono- and pyrophosphate substituents, further separation of the OS-W components was accomplished by gel-filtration chromatography using Bio-Gel P4 (fine). Two overlapping OS-W

fractions were obtained, OS1-W and OS2-W. ^{1}H NMR analysis of the two fractions (Fig. 6) showed that OS1-W was greatly enriched in oligosaccharides that contained a PEA substituent (as evidenced by the PEA–CH_2–NH_3^+ methylene signal at 3.22 ppm) while OS2-W largely lacked PEA. Detailed NMR analysis was done on the OS1-W fraction. The assignments of the various resonances were determined by a series of NMR experiments, including gCOSY, TOCSY, and gHSQC. These assignments are shown in Table 3. The results indicated that the OS1-W fraction consisted of a number of oligosaccharides that differed from one another depending on whether HepI was substituted with pyrophosphate or PPEA. The location of the PPEA group was shown to be present at O-2 of HepI by a ^{31}P–^{1}H HMQC-TOCSY experiment (Fig. 7).

3.4. Analysis of the A-band D-rhamnan from the *galU* mutant

As described above, while the purified LPS, either LPS-PCP or LPS-W, did not contain B-band or A-band glycosyl components, DOC–PAGE immunoblot analysis of the SDS-extract from *galU* mutant cells revealed that it produced material that reacts with antibody to the A-band LPS (Fig. 1B), and was previously shown not react with antibody to the B-band LPS.[18] The difference in electrophoretic mobility between the wild-type and

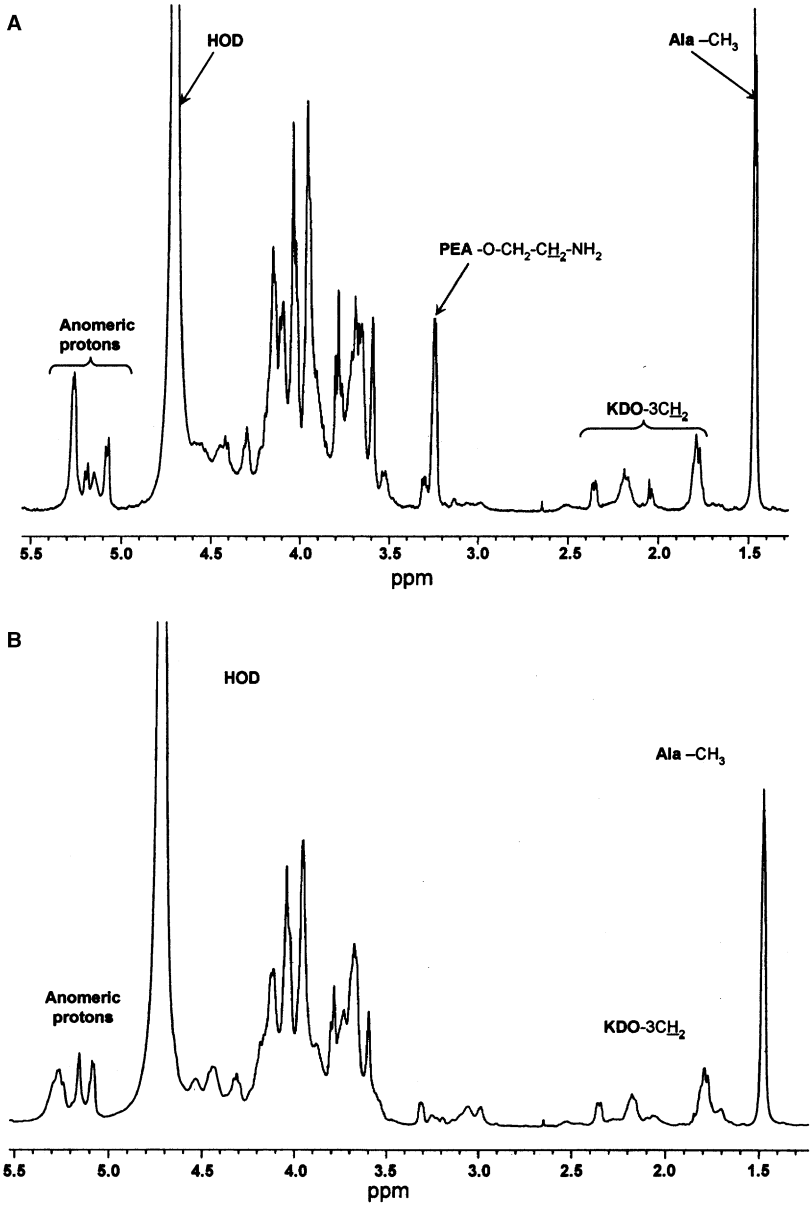

Figure 6. ^{1}H NMR spectra of the OS1-W (A) and OS2-W (B) Bio-Gel P4 fractions showing the separation of PEA-containing (OS1-W) from the non-PEA-containing (OS2-W) fractions.

Table 3. ^{1}H and ^{13}C NMR assignment of the OS1-W fraction[a]

Residue	H-1	H-2	H-3	H-4	H-5	H-6(a,b)	H-7(a,b)	H-8(a,b)
GalNAla	5.27/99.08	4.12/50.83	3.95	3.97	4.06	3.74–3.67		
$HepI_a$	5.26/99.08	4.73/75.21 (PPEA)	4.2	4.42/70.2 (P)	4.15	4.04	3.68, 3.66	
$HepI_b$	5.20/98.73	4.75 (PP)	4.19	4.42/72.8 (P)	4.16	4.04	3.68, 3.67	
$HepI_c$(t)	5.17/103.5	4.65 (P)	—	—	—	—	—	
$HepII_{a,b}$	5.08/103.06	4.31	4.97	3.89	3.99	4.56 (P)	4.51, 3.92	
Kdo			1.81, 2.20	4.04	4.06	3.69	3.76	3.54, 3.51
Ala	1.48 (CH_3)	4.03 (α-CH)						
PPEA	3.26 (CH_2'')	4.16 (CH_2')						

[a] A minor component that contains a Hep residue substituted with monophosphate at O-2 (H-1 is at 5.17/103.5 ppm and H-2 is at 4.55 ppm which, in turn, is connected to a ^{31}P resonance at a −0.1 ppm) is also observed. However, due to the low level of this component, further assignments could not be made.

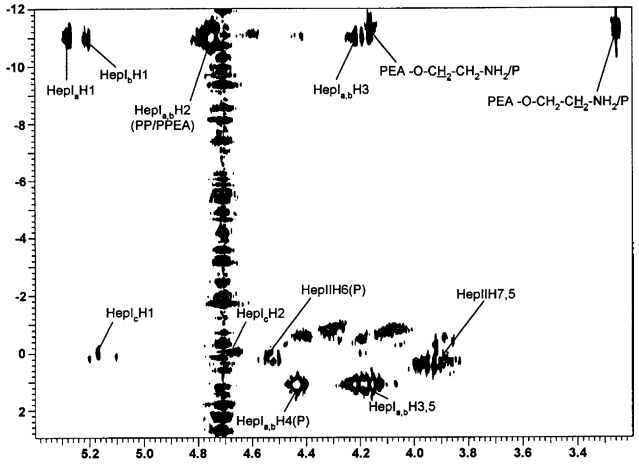

Figure 7. ^{1}H–^{31}P HMQC-TOCSY of the OS1-W fraction. The resonances are assigned as indicated.

mutant A-band material, and the more diffuse nature of the wild-type A-band may be due to the presence of B-band LPS in wild-type LPS preparation or due to the lack of lipid-A and core oligosaccharide components in the mutant A-band (see below). During the purification of LPS-W, the LPS was purified from the aqueous phase of the hot phenol–water extract by sedimentation using ultracentrifugation. Composition analysis of the supernatant showed the presence of Rha, Man, and GlcNAc, and the absence of any detectable fatty acids or typical core oligosaccharide glycosyl residues, indicating that this Rha-containing material was not attached to a core-lipid A structure. Glycosyl linkage analysis showed the presence of 2-linked and 3-linked Rha in a 1:2 ratio with a small amount of terminal rhamnose. In addition, 4-linked Man and 4-linked GlcNAc were detected. The Rha linkages are consistent with the structure of the A-band polysaccharide, and therefore, these results probably explain the presence of anti-A-band reactive material in the *galU* mutant. During its synthesis, the A-band polysaccharide is reported to be linked to O-3 of a GlcNAc, that is, in turn, attached to an undecaprenyl lipid.[30] However, 3-linked GlcNAc was not detected in the A-band polysaccharide from the *galU* mutant; only 4-linked GlcNAc was observed.

The ^{1}H NMR analysis of the isolated and purified A-band material (spectrum not shown) showed the presence of three anomeric protons with chemical shifts of 5.2, 5.04, and 4.98 ppm, respectively, indicating a trisaccharide repeat. The signals for the methyl protons of Rha were also observed at 1.3 ppm, as well as several low-intensity signals around 2.0 ppm, indicating the presence of small amounts of *O*-acetyl and *N*-acetyl substituents. Hence these data confirm the fact that the *galU* mutant synthesizes A-band polysaccharide but that it is not present as A-band LPS; that is, it is not attached to the lipid A/core region of the LPS.

4. Discussion

The mutant strain investigated in this study originated by nonpolar inactivation of the *galU* gene of PA103, a serogroup O11 strain.[18] The *galU* gene encodes UDP-glucose pyrophosphorylase activity that utilizes Glc-1-P and UTP (uridine triphosphate) to synthesize UDP-Glc; a precursor required for LPS-core OS biosynthesis. Hence, the *galU* mutation resulted in LPS-core truncation presumably due to its inability to incorporate Glc into the core region of the LPS. The inability to add Glc to the core region resulted in the expected truncated core consisting of the inner core region of α-GalN(Ala)-(1→3)-α-HepII(7Cm)-(1→3)-α-HepI-(1→5)-Kdo in which the HepI residue contains phosphate, pyrophosphate, pyrophosphoethanolamine, or triphosphate at O-2, phosphate at O-4, and in which HepII can be occasionally monophosphorylated at O-6. These structures are summarized in Figure 8. The glycosyl structure of the LPS from the *galU* mutant is the same as that reported for Δ*algC* mutants of PAO1 and PAC1R, serogroups O5 and O3, respectively, which are defective in the mutase enzyme activities that convert Man-6-phosphate and Glc-6-phosphate into their respective 1-phosphates.[13] However, differences between the PA103 *galU* mutant and the Δ*algC* mutants were observed in the

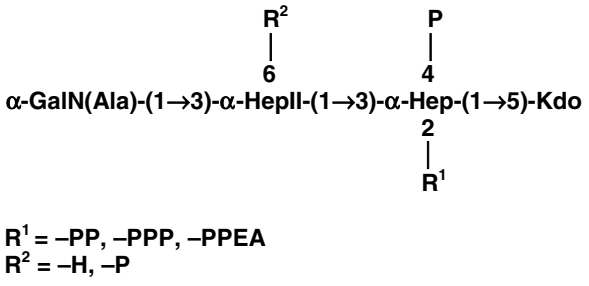

Figure 8. A summary of the LPS oligosaccharide structures found on the PA103 *galU* mutant.

phosphorylation pattern of the inner core region. The Δ*algC* mutants from serogroups O3 and O5 contained up to four phosphate groups, two of which were part of a –PPEA residue attached to O-2 of HepI in the case of the serogroup O5 mutant, with another of the phosphates residing on O-6 of HepII for both mutants.[13] In our case of the PA103 *galU* mutant, the inner core region was more heterogeneous in its phosphorylation pattern containing up to six phosphate groups, including a possible -PPP group. In addition, it was possible to separate oligosaccharides containing –PPEA from those not containing this substituent, and analysis of the –PPEA-containing structure showed that this group was located on O-2 of HepI as was reported for the Δ*algC* mutants. Thus, the *galU* mutant produces truncated LPS with a higher level of phosphorylation, a greater level of heterogeneity in phosphorylation, and the possible presence of a -PPP group on HepI in some molecules. The differences in phosphorylation pattern between the *galU* versus the Δ*algC* mutants could be due to serogroup variation; that is, O3 and O5 for the Δ*algC* mutants versus O11 in the case of the *galU* mutant.

It is not surprising that the PA103 *galU* mutant does not produce B-band LOS since the truncated core region would not serve as an acceptor for the B-band polysaccharide. Likewise, this truncated LOS would also not serve as an acceptor for the A-band polysaccharide. Nevertheless, the A-band polysaccharide was detected using anti-A-band mAb, as well as by chemical analysis. However, this A-band polysaccharide material does not appear to be part of the LPS since no core or lipid-A components were detected. Therefore, it is likely that the A-band polysaccharide is synthesized on its undecaprenol phosphate carrier but cannot be transferred to the truncated core region of the PA101 *galU* mutant LPS, as was reported by Sadovskaya et al.[31] for strains AK1401 and AK1012.

Acknowledgements

This work was supported by NIH Grant AI50230 to J.B.G., and by DOE Grant DE-FG-02-93ER20097 to the CCRC. We gratefully acknowledge the technical assistance of Elizabeth Coleman.

References

1. Pier, G. B.; Grout, M.; Zaidi, T. S.; Olsen, J. C.; Johnson, L. G.; Yankaskas, J. R.; Goldberg, J. B. *Science* **1996**, *271*, 64–67.
2. De Kievit, T. R.; Lam, J. S. *J. Bacteriol.* **1994**, *176*, 7129–7139.
3. Arsenault, T. L.; Huges, D. W.; MacLean, D. B.; Szarek, W. A.; Kropinski, A. M. B.; Lam, J. S. *Can. J. Chem.* **1991**, *69*, 1273–1280.
4. Knirel, Y. A. *Crit. Rev. Microbiol.* **1990**, *17*, 273–304.
5. Yethon, J. A.; Gunn, J. S.; Ernst, R. K.; Miller, S. I.; Laroche, L.; Malo, D.; Whitfield, C. *Infect. Immun.* **2000**, *68*, 4485–4491.
6. Lam, J. S.; MacDonald, L. A.; Kropinski, A. M. B.; Speert, D. P. *Serodiagn. Immunother. Infect. Dis.* **1988**, *2*, 365–374.
7. Preston, M. J.; Fleiszig, S. M.; Zaidi, T. S.; Goldberg, J. B.; Shortridge, V. D.; Vasil, M. L.; Pier, G. B. *Infect. Immun.* **1995**, *63*, 3497–3501.
8. Schroeder, T. H.; Lee, M. M.; Yacono, P. W.; Cannon, C. L.; Gerceker, A. A.; Golan, D. E.; Pier, G. B. *Proc. Natl. Acad. Sci. U.S.A.* **2002**, *99*, 6907–6912.
9. Masoud, H.; Altman, E.; Richards, J. C.; Lam, J. S. *Biochemistry* **1994**, *33*, 10568–10578.
10. Knirel, Y. A.; Bystrova, O. V.; Shashkov, A. S.; Lindner, B.; Kocharova, N. A.; Senchenkova, S. N.; Moll, H.; Zähringer, U.; Hatano, K.; Pier, G. B. *Eur. J. Biochem.* **2001**, *268*, 4708–4719.
11. Bystrova, O. V.; Lindner, B.; Moll, H.; Kocharova, N. A.; Knirel, Y. A.; Zähringer, U.; Pier, G. B. *Carbohydr. Res.* **2003**, *338*, 1895–1905.
12. Bystrova, O. V.; Shashkov, A. S.; Kocharova, N. A.; Knirel, Y. A.; Lindner, B.; Zähringer, U.; Pier, G. B. *Eur. J. Biochem.* **2002**, *269*, 2194–2203.
13. Kooistra, O.; Bedoux, G.; Brecker, L.; Lindner, B.; Carballo, P. S.; Haras, D.; Zähringer, U. *Carbohydr. Res.* **2003**, *338*, 2667–2677.
14. Goldberg, J. B.; Coyne, M. J., Jr.; Neely, A. N.; Holder, I. A. *Infect. Immun.* **1995**, *63*, 4166–4169.
15. Coyne, M. J., Jr.; Russell, K. S.; Coyle, C. L.; Goldberg, J. B. *J. Bacteriol.* **1994**, *176*, 3500–3507.
16. Tang, H. B.; DiMango, E.; Bryan, R.; Gambello, M.; Iglewski, B. H.; Goldberg, J. B.; Prince, A. *Infect. Immun.* **1996**, *64*, 37–43.
17. Priebe, G. P.; Dean, C. R.; Zaidi, T.; Meluleni, G. J.; Coleman, F. T.; Coutinho, Y. S.; Noto, M. J.; Urban, T. A.; Pier, G. B.; Goldberg, J. B. *Infect. Immun.* **2004**, *72*, 4224–4232.
18. Dean, C. R.; Goldberg, J. B. *FEMS Microbiol. Lett.* **2002**, *210*, 277–283.
19. Dean, C. R.; Datta, A.; Carlson, R. W.; Goldberg, J. B. *J. Bacteriol.* **2002**, *184*, 323–326.
20. Galanos, C.; Luderitz, O.; Westphal, O. *Eur. J. Biochem.* **1969**, *9*, 245–249.
21. Westphal, O.; Jann, K. *Methods Carbohydr. Chem.* **1965**, *5*, 83–91.
22. Komuro, T.; Galanos, C. *J. Chromatogr.* **1988**, *450*, 381–387.
23. Tsai, C.; Frisch, C. E. *Anal. Biochem.* **1982**, *119*, 115–119.

24. Dean, C. R.; Franklund, C. V.; Retief, J. D.; Coyne, M. J., Jr.; Hatano, K.; Evans, D. J.; Pier, G. B.; Goldberg, J. B. *J. Bacteriol.* **1999**, *181*, 4275–4284.
25. Lam, M. Y. C.; McGroarty, E. J.; Kropinski, A. M.; MacDonald, L. A.; Pederson, S. S.; Høiby, N.; Lam, J. S. *J. Clin. Microbiol.* **1989**, *27*, 962–967.
26. Knirel, Y. A.; Helbig, J. H.; Zähringer, U. *Carbohydr. Res.* **1996**, *283*, 129–139.
27. York, W. S.; Darvill, A. G.; McNeil, M.; Stevenson, T. T.; Albersheim, P. *Methods Enzymol.* **1985**, *118*, 3–40.
28. Ciucanu, I.; Kerek, F. *Carbohydr. Res.* **1984**, *131*, 209–217.
29. Maurien, M. A. O.; Johan, H.; Thomas-Oates, J. E. *J. Mass Spectrom.* **1999**, *34*, 622–636.
30. Overa, C.; Goldberg, J. B.; Sanchez, R.; Soberon-Chavez, G. *FEMS Microbiol. Lett.* **1999**, *179*, 73–78.
31. Sadovskaya, I.; Brisson, J. R.; Lam, J. S.; Richards, J. C.; Altman, E. *Eur. J. Biochem.* **1998**, *255*, 673–684.
32. Olsthoorn, M. M. A.; Haverkamp, J.; Thomas-Oates, J. E. *J. Mass Spectrom.* **1999**, *34*, 622–636.